Supplementary Material

Heterostructured *n*-ZnO@*p*-CuO nanosheets filled in polymer matrix for enhanced electrostatic energy storage performance

Weixuan Zhang, Yuqing Hu, Xin Zhang, Yingda Zhang, Jinzhang Liu*

School of Materials Science and Engineering, Beihang University, Beijing 100191, China.

**Corresponding author.*

E-mail Address: J. Z. Liu (ljz78@buaa.edu.cn).

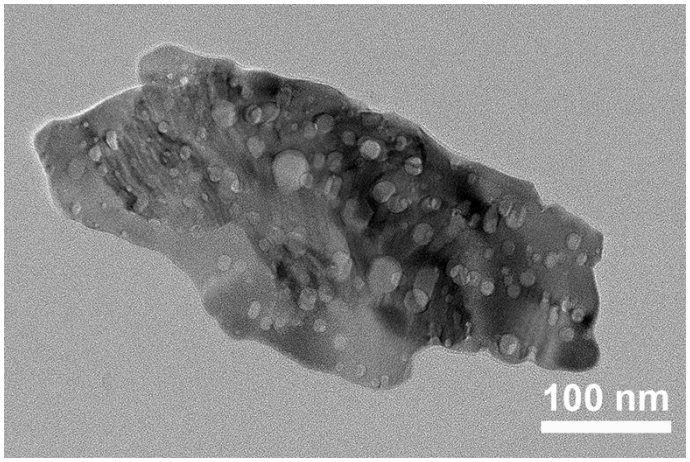

Fig. S1. TEM image of a single ZnO nanosheet.

Fig. S2a, b, and c show high-resolution XPS Zn 2p, Cu 2p, and O 1s spectra collected from ZnO@CuO nanosheets. In Fig. S2a, two Zn 2p peaks at 1021.4 eV and 1044.5 eV are identified as Zn-O bonds of Zn^{2+} in ZnO. In Fig. S2b, the two peaks at 933.1 eV and 952.2 eV are fitted with Cu $2p_{3/2}$ and Cu $2p_{1/2}$ respectively, and the peaks at 961.9–962.3eV and 940.5-943.7 eV are the satellite peaks of CuO[S1]. In Fig. S2c, two peaks at 530.3 eV and 532.3 eV are related to metal-oxygen bonds in ZnO and CuO.

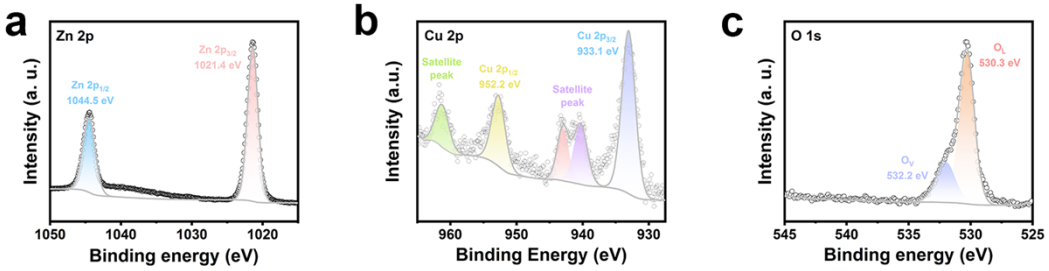

Fig. S2. High-resolution (a) Zn 2p, (b) Cu 2p, and (c) O1s XPS spectra of ZnO@CuO nanosheets.

Fig. S3 exhibits the cross-sectional SEM images of ZnO@CuO/P(VDF-HFP) nanocomposites with different filler contents. The average thickness of the films is

about 15 μm, and the fillers were uniformly distributed in the polymer matrix without obvious agglomeration.

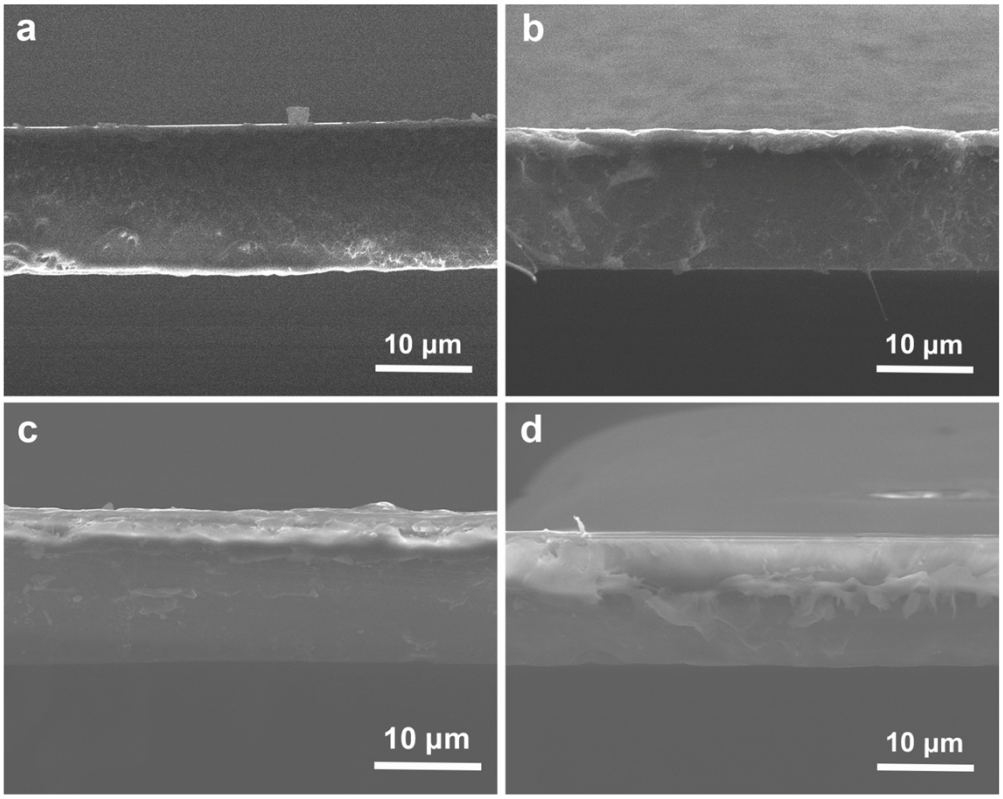

Fig. S3. Cross-sectional SEM images of ZnO@CuO/P(VDF-HFP) nanocomposites with (a) 1 wt%, (b) 3 wt%, (c) 5 wt%, and (d) 7 wt% ZnO@CuO nanosheets.

Fig. S4 shows the phase contents of pure P(VDF-HFP) and ZnO@CuO/P(VDF-HFP) films filled with different filler contents. The relative fraction of γ phase can be calculated by:

$$F(\gamma) = \frac{A_\gamma}{(K_\gamma/K_\alpha)A_\alpha + A_\gamma} \quad \text{(S1)}$$

Where A_γ and A_α are the absorption intensities of γ and α phases at 835 and 763 cm^{-1}, respectively; K_γ and K_α are the absorption coefficients at the respective wavenumber, which are 7.7×10^4 and 6.1×10^4 cm^2/mol, respectively.[S2]

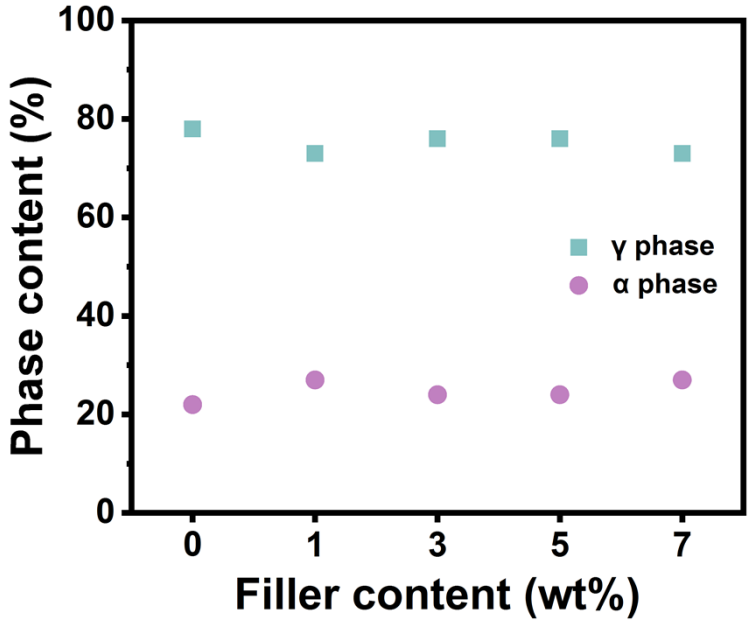

Fig. S4. Contents of α and γ phases in pure P(VDF-HFP) and ZnO@CuO/P(VDF-HFP) films with different filler contents.

Fig. S5 shows the variations of dielectric constant and dielectric loss with increasing the frequency for pure P(VDF-HFP) and ZnO/P(VDF-HFP) nanocomposites with different filler contents. With increasing the filler content from 0 to 5wt%, the dielectric constant and loss were increased slowly. However, the two parameters were abruptly increased when the filler content reaches 7 wt%. It implies that the use of ZnO nanosheet filler requires a larger content to enhance the dielectric constant.

Fig. S6 shows the Weibull distribution of electric breakdown strength of pure P(VDF-HFP) and ZnO/P(VDF-HFP) nanocomposites with different filler contents. Compared with the pure P(VDF-HFP), the breakdown strengths of the nanocomposites were slightly improved, and then decreased. The film with filler

content of 1 wt% exhibits the largest breakdown strength among the ZnO/P(VDF-HFP) nanocomposites.

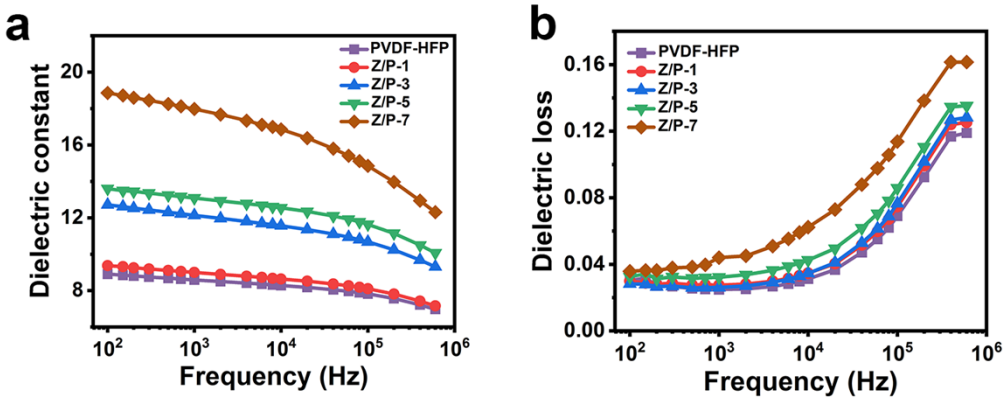

Fig. S5. Dependences of (a) dielectric constant and (b) dielectric loss on frequency for pure P(VDF-HFP) and ZnO/P(VDF-HFP) nanocomposites with different filler contents.

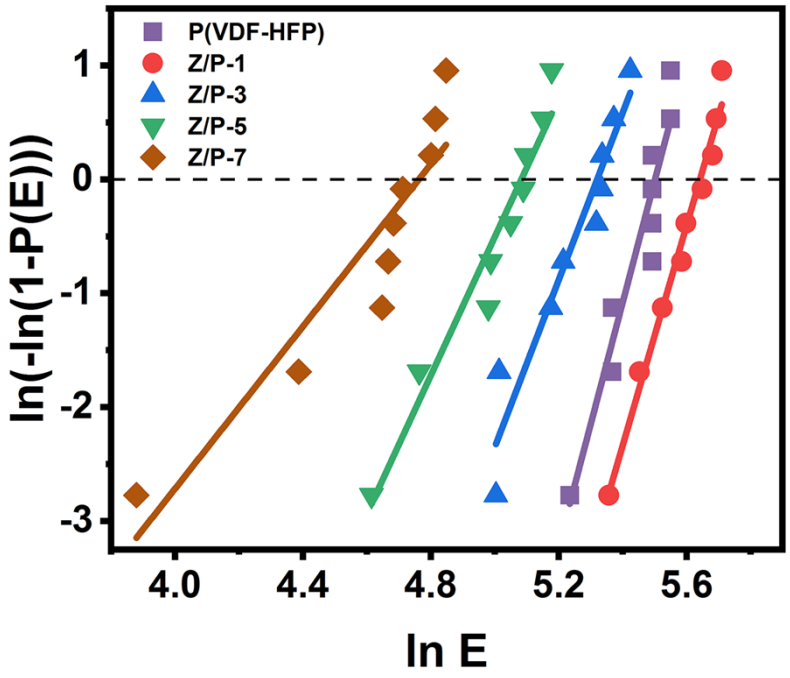

Fig. S6. Weibull distribution of electric breakdown strength of pure P(VDF-HFP) and ZnO/P(VDF-HFP) nanocomposites with different filler content.

In Fig. S7, the D-E loops were collected from a pure P(VDF-HFP) film. The electric breakdown strength of a P(VDF-HFP) film is around 200 MV m^{-1}. In addition, more D-E loops were collected from ZnO@CuO/P(VDF-HFP) films with filler contents ranging from 1 wt% to 7 wt%, as shown in Fig. S8. The use of 3 wt% filler content leads to the highest electric breakdown strength. For further comparison, D-E loops collected from a group of ZnO/P(VDF-HFP) films are shown in Fig. S9.

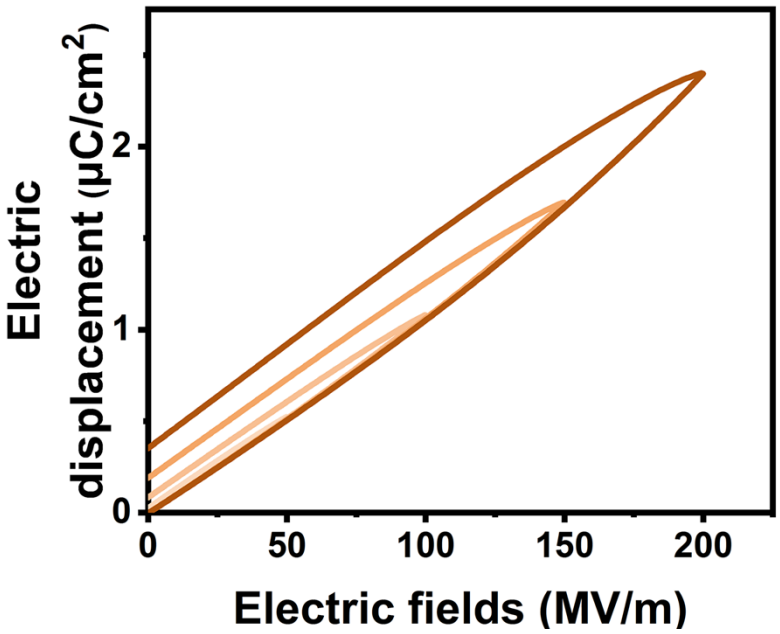

Fig. S7. D-E loops of pure P(VDF-HFP) at different electric fields.

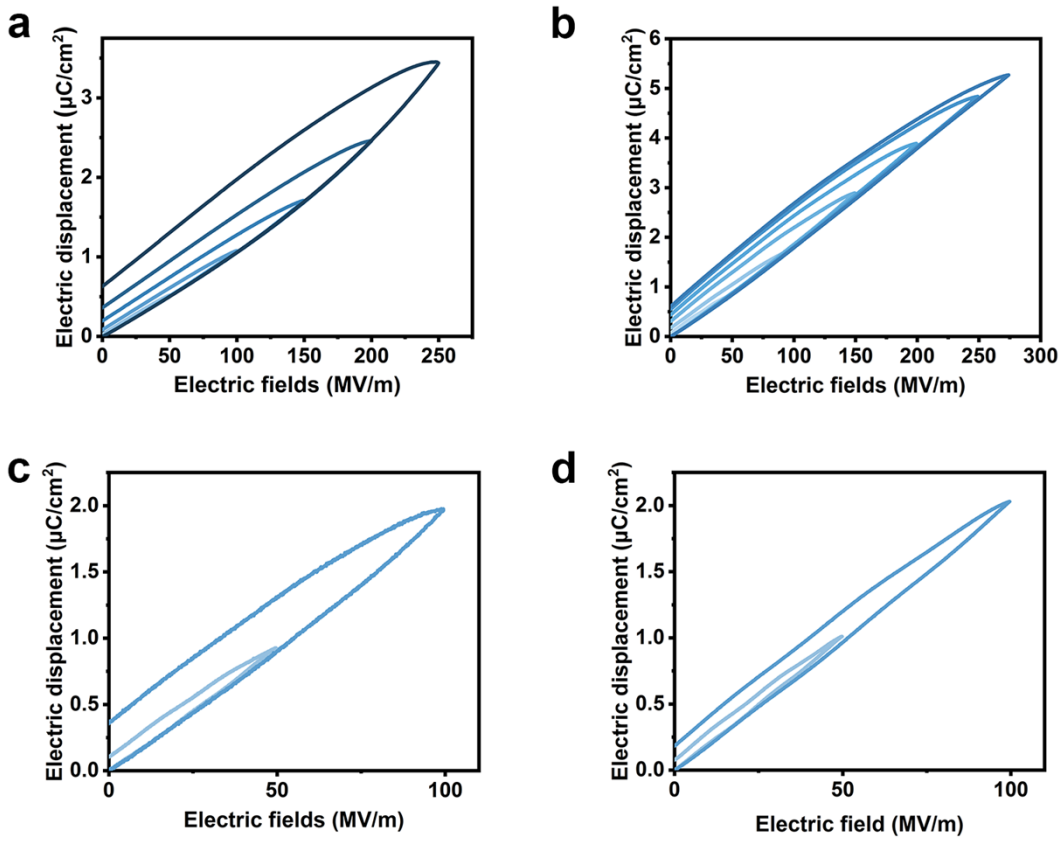

Fig. S8. D-E loops of ZnO@CuO/P(VDF-HFP)nanocomposites with (a) 1 wt%, (b) 3 wt%, (c) 5 wt%, and (d) 7 wt% filler content at different electric fields.

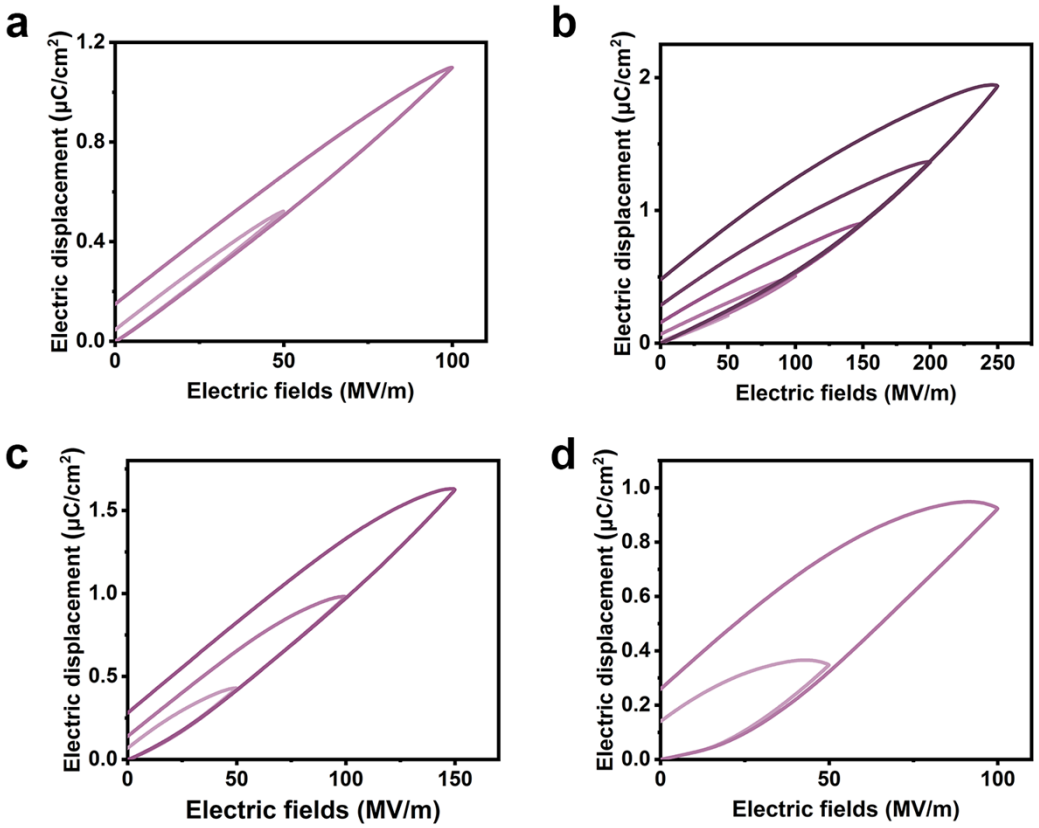

Fig. S9. D-E loops of ZnO/P(VDF-HFP)nanocomposites with (a) 1 wt%, (b) 3 wt%, (c) 5 wt%, and (d) 7 wt% filler content at different electric fields.

Fig. S10 exhibits the dielectric energy storage properties of ZnO/P(VDF-HFP) nanocomposites with different filler content. Fig. S10a shows dependences of discharged energy density U_d and charge-discharge efficiency η on the electric filed strength for ZnO/P(VDF-HFP) films. The film with filler content of 3 wt% exhibits largest highest U_d of 1.48 J cm^{-3} at 250 MV m^{-1} with η of 52% among the ZnO/P(VDF-HFP) nanocomposites. Fig. S10b shows dependences of maximum and remnant electric displacements on the ZnO nanosheet content and the ZnO/P(VDF-HFP) composite film with 3 wt% filler content exhibits the highest (D_{max} - D_r), as

1.46 μC cm^{-2}. The results of calculated C_{loss} and F_{loss} for ZnO/P(VDF-HFP) films are shown in Fig. S10c and d, respectively.

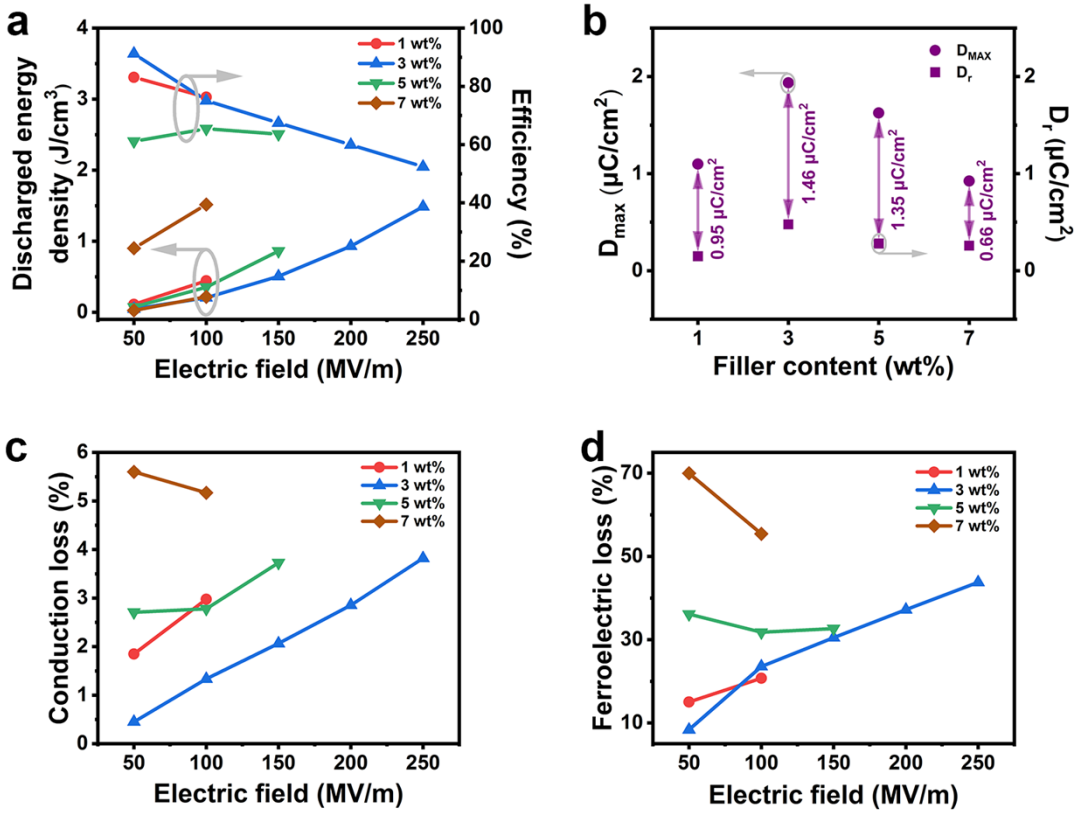

Fig. S10. (a) Discharged energy density U_d and efficiency η, (b) maximum and remnant electric displacement, (c) conduction loss, and (d) ferroelectric loss of ZnO/P(VDF-HFP) nanocomposites with different filler content.

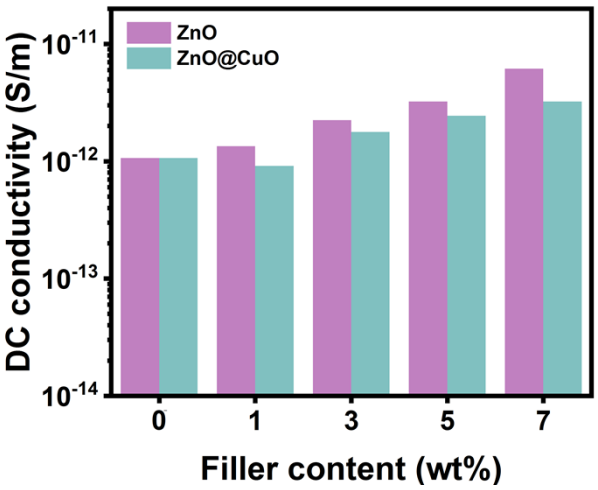

Fig. S11. Electrical conductivities of ZnO/P(VDF-HFP) and ZnO@CuO/P(VDF-HFP) composite films with different filler contents.

References

[S1] X. Liu, X. Lu, H. Guan, X. Liu, Y. Wang, D. Zhao and M. Wang, Ceram. Int., 2022, 48, 6948–6955.

[S2] R. Gregorio, and M. Cestari, J. Polym. Sci. Part B Polym. Phys., 1994, 32, 859–870.